AFCRL-65-68

DETERMINATION OF THE SHAPE OF A FREE BALLOON

Cylinder, Cylinder-End, Taper-Tangent, and Tangent-Harness Balloons

by

Justin H. Smalley

APPLIED SCIENCE DIVISION
Litton Systems, Inc.
2295 Walnut Street
St Paul, Minnesota 55113

Report No 2671

Contract No. AF 19(628)-2783

Project No. 6665

Task No. 666501

Scientific Report No. 4

1 November 1964

Prepared for:

AIR FORCE CAMBRIDGE RESEARCH LABORATORIES
OFFICE OF AEROSPACE RESEARCH
UNITED STATES AIR FORCE
BEDFORD, MASSACHUSETTS

ABSTRACT

Modifications of the basic balloon-shape equations are developed for cylinder and cylinder-end balloons, taper-tangent balloons, and tangent-harness balloons. Examples of the shape of these balloons are presented, and corresponding meridional stresses are determined. Zero and non-zero circumferential stresses are considered.

TABLE OF CONTENTS

LIST OF ILLUSTRATIONS

DETERMINATION OF THE SHAPE OF A FREE BALLOON

Scientific Report No. 4

I. INTRODUCTION

In a previous report[1] the general equations were developed for determining the shapes and stresses of axi-symmetric balloons. In succeeding reports[2, 3] examples of various balloon types were presented. In this report three additional types of balloons will be considered: 1) balloons with cylinder-end sections, including those completely cylindrical; 2) balloons with taper-tangent end sections; and 3) balloons with the payload attached by a tangent-cone harness.

II. GENERAL EQUATIONS AND SOLUTION

The general equations[1] for the shape and stresses of a balloon are

$$\left.\begin{aligned} \frac{d\Theta}{ds} &= \left[t_c\, z' - w\, r\, r' - b\, r(z + a)\right]/(r\, t_m) \\ \frac{d(r\, t_m)}{ds} &= t_c\, r' + w\, r\, z', \end{aligned}\right\} \qquad (1)$$

and

$$r' = \sin\Theta$$

$$z' = \cos\Theta,$$

where the prime refers to differentiation with respect to gore position parameter (s). The symbols used throughout this report are defined in Appendix I. The equations in (1) are derived respectively from summations of the forces normal and parallel to an elemental rectangular area of the balloon surface. These equations are restricted to balloons made from thin, flexible, inelastic material; they may be solved numerically by the Runge-Kutta method. The solution is started at the bottom of the balloon where the payload is attached. An estimate is made of the bottom apex angle. The initial meridional stress (t_m) is thereby determined, since

$$r_o\, t_{m_o} = \frac{L}{2\pi \cos \Theta_o}.$$

The value of the circumferential stress (t_c) may be specified as desired. Values of the variables are determined by successively incrementing s. The solution is complete when the balloon shape closes at the top.

Several methods have been presented[2, 3] for determining the balloon weight and volume. It has since been found that a superior method includes the differential expressions for weight and volume as part of the above set of simultaneous equations defining the balloon shape. The equations to be included are

$$\frac{dA}{ds} = 2\pi r$$

$$\frac{dV}{ds} = \pi r^2 z'.$$

As the total number of gore increments is increased, the volume and area converge to final values about as rapidly as the balloon coordinates converge.

III. MODIFIED EQUATIONS

A. Cylinder and Cylinder-End Balloons

Figure 1 shows what the shape of a cylinder-end balloon would be if all the material were fully deployed.

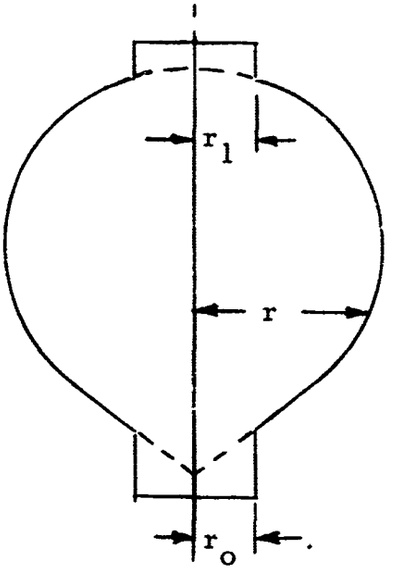

Figure 1. Sketch of cylinder-end balloon with end sections opened

A cylinder balloon is treated as a cylinder-end balloon whose cylindrical portions meet. Except for the cylindrical portions, the balloon is fully tailored and has a constant material unit weight. The cylinder ends are treated as portions of a natural-shaped balloon which have a varying material unit weight. When r is less than r_o (in Figure 1), the weight of an elemental circumferential band of width (ds) is clearly

$$w(2\pi r_o)\, ds.$$

(This weight and the expressions that follow are the same in the upper end section except that r_o is replaced by r_1.)

Then the effective weight per unit area is

$$\frac{w(2\pi r_c)\,ds}{2\pi r\,ds} = w(r_o/r).$$

By replacing w in Equations (1), we have in the cylinder-end sections:

$$\left.\begin{aligned} \frac{d\Theta}{ds} &= \left[t_c\, z' - w(r_o)\, r' - b\, r\, (z + a)\right]/(r\, t_m) \\ \frac{d(r\, t_m)}{ds} &= t_c\, r' + w(r_o)\, z'. \end{aligned}\right\} \qquad (1a)$$

The form of r', z', and $\frac{dV}{ds}$ is unchanged, but the area equation becomes

$$\frac{dA}{ds} = 2\pi r_o.$$

To find r_o, it is necessary to specify the initial meridional stress (t_{m_o}). The total film load is

$$T_o = L/\cos\Theta_o = 2\pi r_o\, t_{m_o},$$

so

$$r_o = L/(2\pi\, t_{m_o} \cos\Theta_o).$$

The initial meridional stress is known from material strength considerations. As s is being incremented, the stress will exceed its original value because of the material weight. When $r = r_o$, the shape equations revert to the form of Equations (1). Finally, when t_m reaches a second predetermined value, Equations (1a) are used again with r_o replaced by r_1.

B. Taper-Tangent Balloons

As was the case for cylinder-end balloons, it is helpful to examine the shape of a taper-tangent balloon as if all the material were fully deployed (see Figure 2).

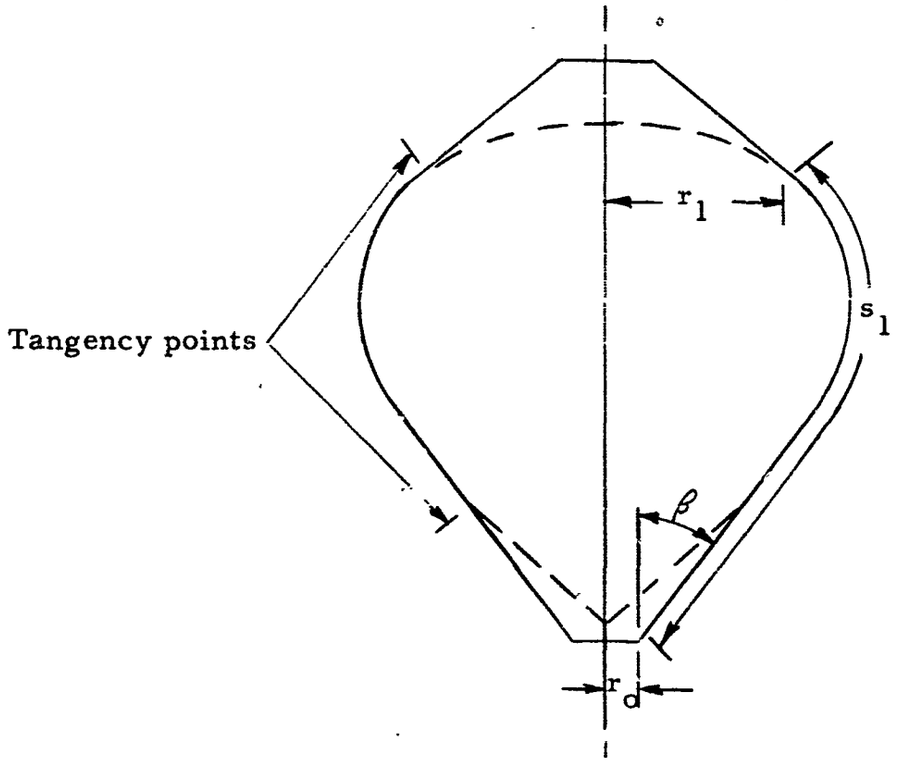

Figure 2. Sketch of taper-tangent balloon with end sections opened (Note: $s_o = 0$)

In Figure 2, it is also clear that in the areas where there is fullness due to the taper-tangent end section, the weight of an elemental band of width (ds) is

$$w(2\pi)\left[r_o + (s - s_o)\sin\beta\right] ds .$$

*In the lower end section r_o and s_o are used; in the upper end section r_1 and s_1 are used.

The modified shape equations are then

$$\left.\begin{aligned} \frac{d\Theta}{ds} &= \left[t_c\, z' - w\left\{ r_o + (s - s_o)\sin\beta \right\} r' - b\, r\, (z + a) \right] / (r\, t_m) \\ \frac{d(r\, t_m)}{ds} &= t_c\, r' + w\left\{ r_o + (s - s_o)\sin\beta \right\} z' . \end{aligned} \right\} \quad (1b)$$

The area equation is

$$\frac{dA}{ds} = 2\pi\left\{ r_o + (s - s_o)\sin\beta \right\}.$$

Balloon shapes of this type are computed in much the same way as the balloon shapes of cylinder-end types. The angle β may be initially specified as zero. The actual value is then found by iterative trial and error. After r passes its maximum and after t_m reaches a specified value, β is set to equal Θ; r_o becomes r_1, s_o becomes s_1, and the shape equations used change from the form of Equations (1) to that of Equations (1b).

C. Tangent-Harness Balloon

In previous reports and up to this time, all payloads have been considered to be applied at the axis of symmetry. For the tangent-harness balloon, the payload is attached at a circumferential ring. There are several ways this can be done. The particular method we have chosen herein applies the payload tangentially. There is a discontinuity in meridional stress and in radius of curvature at the ring, but no discontinuity in the slope of the shape curve. The balloon is approximately spherical below that point. The method used to compute the balloon shape depends upon the circumferential stress. Two stress conditions are discussed below: meridional and circumferential stress equal; and circumferential stress equal to zero.

1. Meridional and Circumferential Stress Equal

If $t_c = t_m$, Equations (1) may be modified and simplified. By replacing t_c with t_m, the first of Equations (1) becomes

$$\frac{d\Theta}{ds} = \frac{z'}{r} - \frac{w\,r' + b(z + a)}{t_m}.$$

If the left-hand side of the second of Equations (1) is differentiated,

$$\frac{d(r\,t_m)}{ds} = t_m\,r' + r\,t_m',$$

and is set equal to the right-hand side, rearranged, and integrated, then

$$t_m = w\,z + t_{m_o}.$$

For initial values, note that at the bottom of the balloon, $\Theta_o = 90°$ and $R_c = R_m$; then

$$ba + w = \frac{t_c}{R_c} + \frac{t_m}{R_m} = 2\,t_{m_o}/R_{m_o};$$

or initially,

$$\frac{d\Theta}{ds} = \frac{-1}{R_{m_o}} = -\frac{ba + w}{2\,t_{m_o}},$$

where a, w, and t_{m_o} are specified.

During computation it is more convenient to use the differential form of t_m. Then,

$$\left.\begin{aligned} \frac{d\Theta}{ds} &= \frac{z'}{r} - \frac{w\,r' + b(z+a)}{t_m} \\ \frac{d\,t_m}{ds} &= w\,z'. \end{aligned}\right\} \qquad (1c)$$

These equations are integrated from the bottom upward until a specified payload attachment point is reached. At that point t_m is increased by

$$L/(2\pi\, r \cos\Theta).$$

The computation is continued until the balloon closes at the top. To yield a flat-topped balloon, the proper a, t_{m_o}, and harness attachment for a given w are found by trial and error.

2. Circumferential Stress Equal to Zero

If $t_c = 0$, Equations (1) become

$$\left.\begin{aligned} \frac{d\Theta}{ds} &= -\left[w\,r' + b(z+a)\right]/t_m \\ \frac{d(r\,t_m)}{ds} &= w\,r\,z'. \end{aligned}\right\} \qquad (1d)$$

Note that this case is not quite as 'simple' as the case where $t_c = t_m$, because the second equation does not now integrate directly. The initial value of $\frac{d\Theta}{ds}$ is

$$-\frac{w + ba}{t_{m_o}}.$$

Note that this value is twice as large as the initial value when $t_c = t_m$. The initial values of $d(r\,t_m)/ds$ and $r\,t_m$ are zero.

By differentiating $r\,t_m$,

$$\frac{d(r\,t_m)}{ds} = r'\,t_m + r\,t_m',$$

we see that

$$t_m' = w\,z' - \frac{r'\,t_m}{r} \equiv w\cos\Theta - t_m\,(\sin\Theta)/r; \qquad (2)$$

and for t_m finite,

$$\lim_{r \to 0} t_m' \to -\infty \text{ at the bottom}$$

$$\to +\infty \text{ at the top.}$$

This result could have been anticipated from the previous findings for zero-circumferential stress, natural-shaped free balloons.[3] At the top, not only t_m' but t_m approaches infinity, because $r\,t_m$ at the top is finite when $r = 0$.

When these equations are used to find balloon shapes, observe certain precautions: First, it is not possible to start at the top or the bottom and use Equation (2) because of its infinite character. Therefore, it is necessary to use Equations (1d). Secondly, at each point on the balloon there must be correspondence between $r\,t_m$ and t_m. If t_{m_o} is finite, $(r\,t_{m_o})$ is zero. At the outset $r\,t_m$ will change very little; during the numerical evaluation t_m will tend to be a very small value rather than the specified value t_{m_o}. This will cause $d\Theta/ds$ to be unrealistically large. However, by initializing $r\,t_m$ at an arbitrary finite value, the numerical

integration will proceed smoothly. This amounts to specifying t_m at a small but non-zero radius r; t_m will now be infinite at the bottom when $r = 0$. For the balloon designs which would use the tangent-harness concept, it is not desirable to use the material fullness and special end fittings required to accommodate the extra-high stress. Therefore, the shapes of such balloons, where $t_c = 0$, will not be presented.

IV. NON-DIMENSIONAL EQUATIONS

The equations in Section III are most easily used by reducing them to non-dimensional form. This is done by using the proper combinations of b (the unit buoyancy of the lifting gas) and λ (a length proportional to the volume of gas required to lift the payload alone). The results will then be independent of the altitude, the lifting gas used, and the payload. The non-dimensional equations are listed in Table 1 and the symbols are defined in Appendix I. The differential equation for volume is

$$\frac{d}{d\sigma}\left(\frac{V}{\lambda^3}\right) = \pi \int \rho^2 \xi' .$$

Volume and weight are related:

$$b\,V = P + W$$

or

$$\frac{V}{\lambda^3} = 1 + \frac{W}{P} .$$

The weight is

$$\frac{W}{P} = k \sum (A/\lambda^2) .$$

Remember that the area used for balloon weight is the surface area of the balloon material--not the area developed by rotation of the balloon shape.

Table 1. Non-Dimensional Forms of the Balloon Shape and Area Equations*

Fully Tailored Part

$$\frac{d\theta}{d\sigma} = \left[\tau\xi' - k\Sigma\varsigma\varsigma' - \varsigma(\xi + \alpha)\right] / (\varsigma\tau_m)$$

$$\frac{d(\varsigma\tau_m)}{d\sigma} = \tau\varsigma' + k\Sigma\varsigma\xi'$$

$$\frac{d}{d\sigma}\left(\frac{A}{\lambda^2}\right) = 2\pi\varsigma.$$

Cylinder-End Part

$$\frac{d\theta}{d\sigma} = \left[\tau\xi' - k\Sigma\varsigma_o\varsigma' - \varsigma(\xi + \alpha)\right] / (\varsigma\tau_m)$$

$$\frac{d(\varsigma\tau_m)}{d\sigma} = \tau\varsigma' + k\Sigma\varsigma_o\xi'$$

$$\frac{d}{d\sigma}\left(\frac{A}{\lambda^2}\right) = 2\pi\varsigma_o.$$

Taper-Tangent-End Part

$$\frac{d\theta}{d\sigma} = \left[\tau\xi' - k\Sigma\left\{\varsigma_o + (\sigma - \sigma_o)\sin\beta\right\}\varsigma' - \varsigma(\xi + \alpha)\right] / (\varsigma\tau_m)$$

$$\frac{d(\varsigma\tau_m)}{d\sigma} = \tau\varsigma' + k\Sigma\left\{\varsigma_o + (\sigma - \sigma_o)\sin\beta\right\}\xi'$$

$$\frac{d}{d\sigma}\left(\frac{A}{\lambda^2}\right) = 2\pi\left\{\varsigma_o + (\sigma - \sigma_o)\sin\beta\right\}.$$

---

*Note: In this table, $\varsigma' = \sin\theta$ and $\xi' = \cos\theta$.

Table 1. Non-Dimensional Forms of the Balloon Shape and Area Equations (Continued)

Tangent-Harness Design ($t_c = 0$)

$$\frac{d\theta}{d\sigma} = -\left[k\Sigma\,\varsigma' + \xi + \alpha\right]/\tau_m$$

$$\frac{d(\varsigma\,\tau_m)}{d\sigma} = k\Sigma\,\varsigma\,\xi'.$$

Tangent-Harness Design ($t_c = t_m$)

$$\frac{d\theta}{d\sigma} = \frac{\xi'}{\varsigma} - \frac{k\Sigma\,\varsigma' + \xi + \alpha}{\tau_m}$$

$$\frac{d\,\tau_m}{d\sigma} = k\Sigma\,\xi'.$$

V. RESULTS

A great deal of effort and computer time have been required to find solutions to the equations in Section IV. The existence of an equation does not imply the existence of a solution. In each case it has been possible to find solutions; but the search for the proper combination of parameters has been tedious and at times frustrating.

In the following paragraphs all the results are non-dimensional. When applying these or other previously tabulated results to an actual case, note the following: From the definition of Σ,

$$b = w/k\Sigma\lambda.$$

From the definition of τ_m,

$$b = t_{m_o}/\tau_{m_o}\lambda^2.$$

By equating, we find that

$$\lambda = \left(\frac{k\Sigma}{\tau_{m_o}}\right)\left(\frac{t_{m_o}}{w}\right).$$

Since

$$P = b\lambda^3,$$

a load-altitude curve can be calculated for a given Σ, τ_{m_o}, and (t_{m_o}/w). For example, for polyethylene at 400 psi stress, (t_{m_o}/w) is approximately constant at 987 feet for all sigmas.

In all cases one of the boundary conditions has been that the balloon shape must close with a horizontal tangent at the top.

A. Cylinder and Cylinder-End Balloons

1. Circumferential Stress Equal to Zero

Figure 3 shows the shape of a cylinder-end balloon when sigma varies and when the initial stress is constant. A value of $\tau_{m_o} = 3.0$ was chosen so a sigma as large as 1.0 could be used. For lesser values ($\tau_{m_o} = 1.0$) there is no solution when sigma is as large as 1.0. Corresponding results for meridional stress are given in Figure 4. By comparing Figures 3 and 4 we can see that the shape changes at the top from fully tailored to cylindrical when τ_m exceeds 3.0. This is an arbitrary value chosen to maintain approximately the same stress value in both cylindrical ends.

The effect of changing the initial meridional stress for a constant sigma is shown in Figures 5 and 6. The dashed lines show the shape of the cylinder ends. Again the change to a cylinder occurs at the top when the initial stress value is reached. For the example chosen ($\Sigma = 0.2$) the balloon becomes a full cylinder when τ_{m_o} is slightly larger than 0.4. When $\tau_{m_o} = 0.4$, the cylinder radius is greater than the maximum radius of the balloon shape; so in effect sigma is slightly larger than the initially specified value.

Gore lengths and weights of various cylinder-end balloons are shown in Figures 7, 8, and 9.

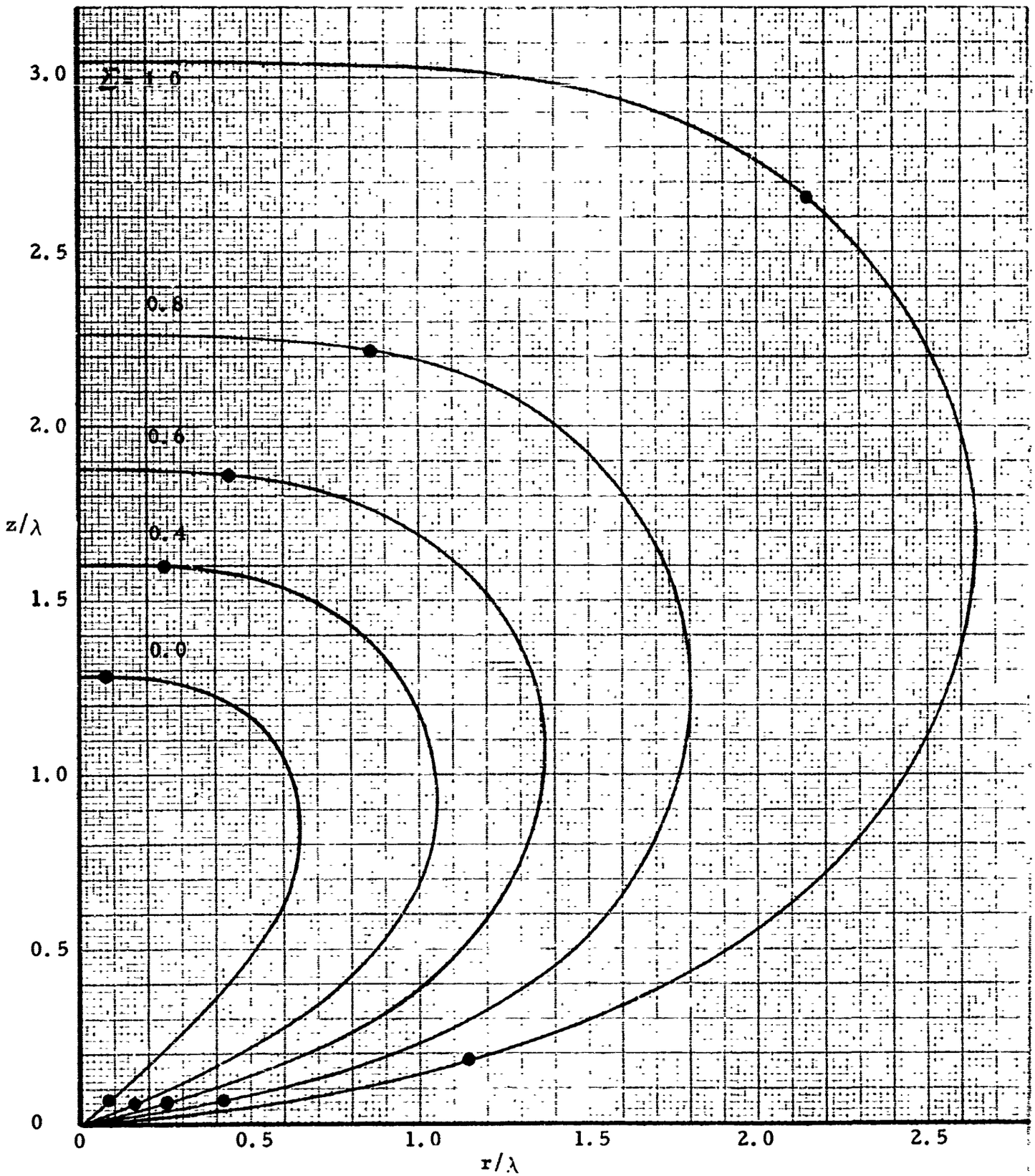

Figure 3. Shapes of balloons with cylindrical end sections and an initial stress value of 3.0 (Zero superpressure, zero circumferential stress)

(Note: The dots indicate the boundary between the cylinder-end and the fully tailored part.)

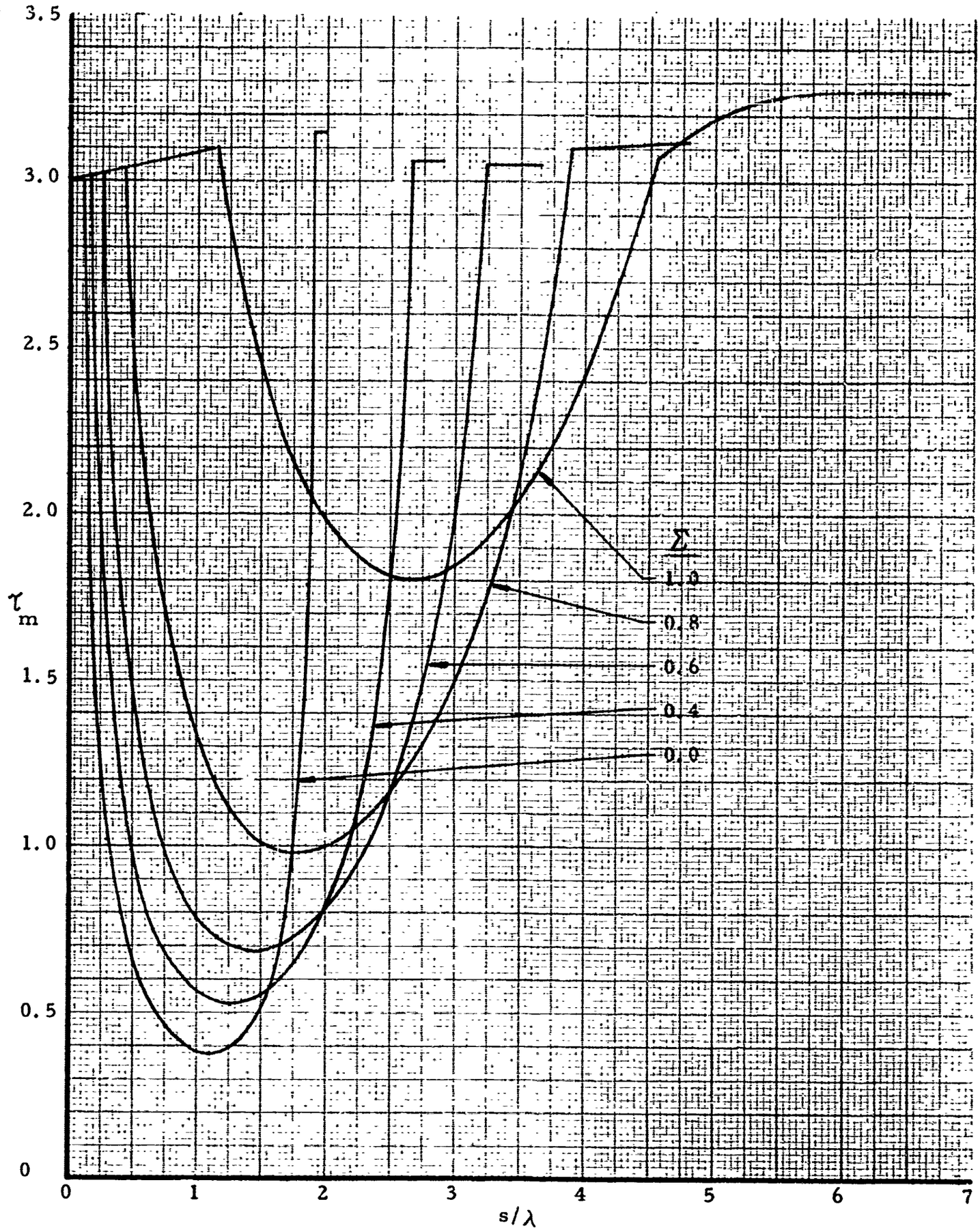

Figure 4. Meridional stress in cylinder-end balloons with an initial stress value of 3.0 (Zero superpressure, zero circumferential stress)

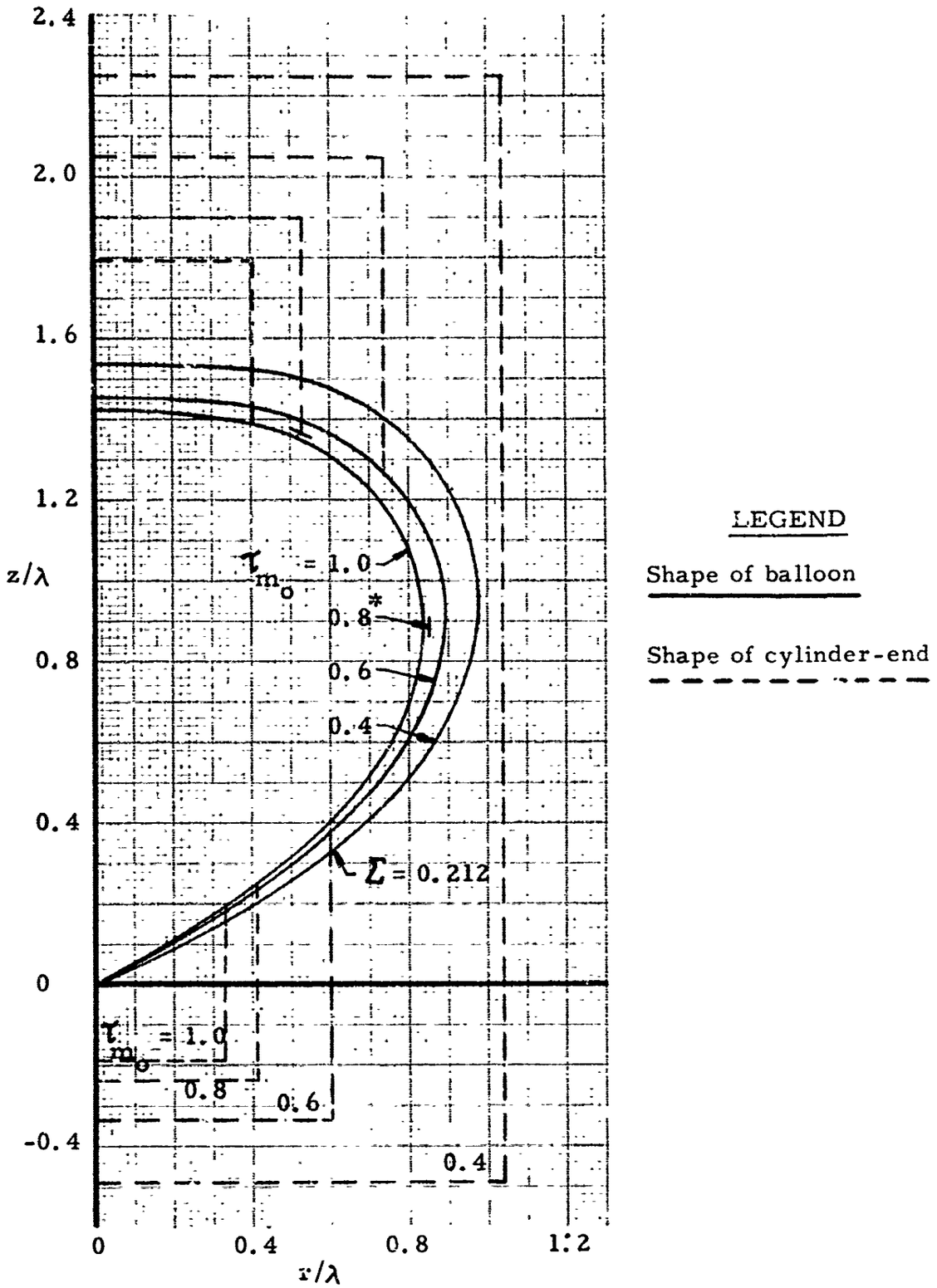

Figure 5. Shapes of balloons with cylindrical-end sections and varying initial stress
(Zero superpressure, zero circumferential stress, $\Sigma = 0.2$)

*(Note: The shape for $\tau_{m_o} = 0.8$ is omitted for clarity.)

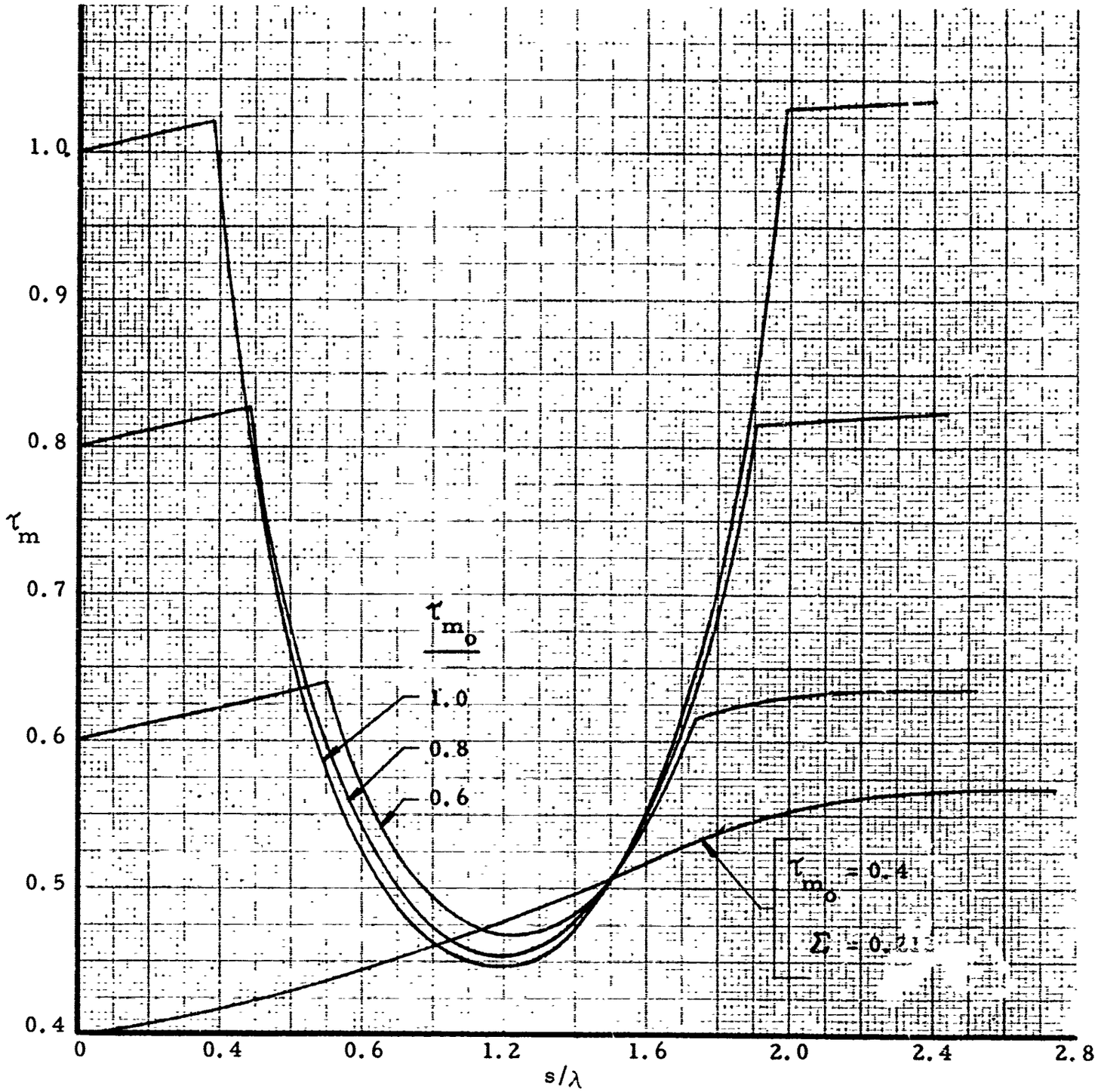

Figure 6. Meridional stress in cylinder-end balloons with varying initial stress (Zero superpressure, zero circumferential stress, $\Sigma = 0.2$)

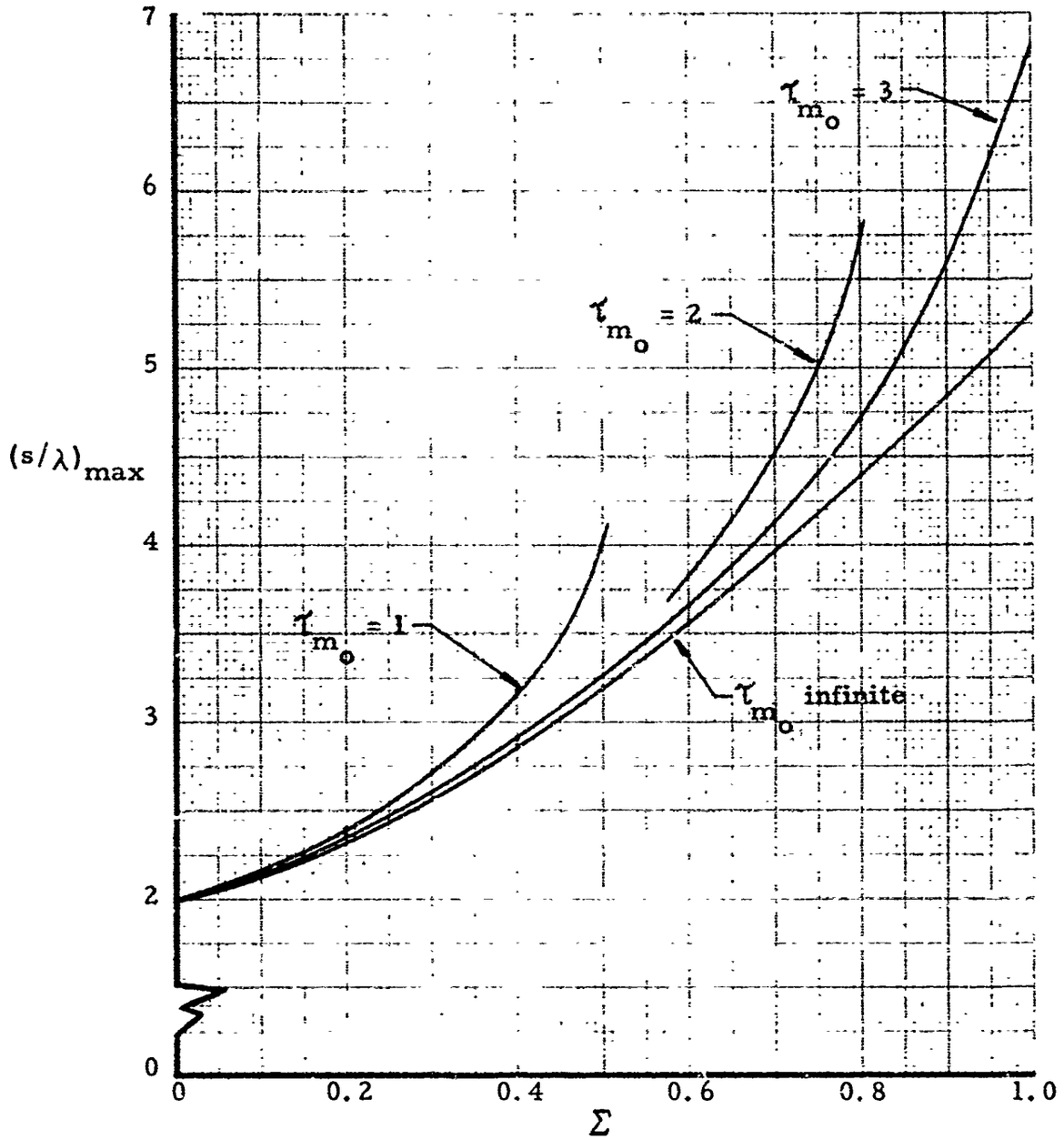

Figure 7. Gore length of cylinder-end balloons with various values of initial meridional stress
(Zero superpressure, zero circumferential stress)

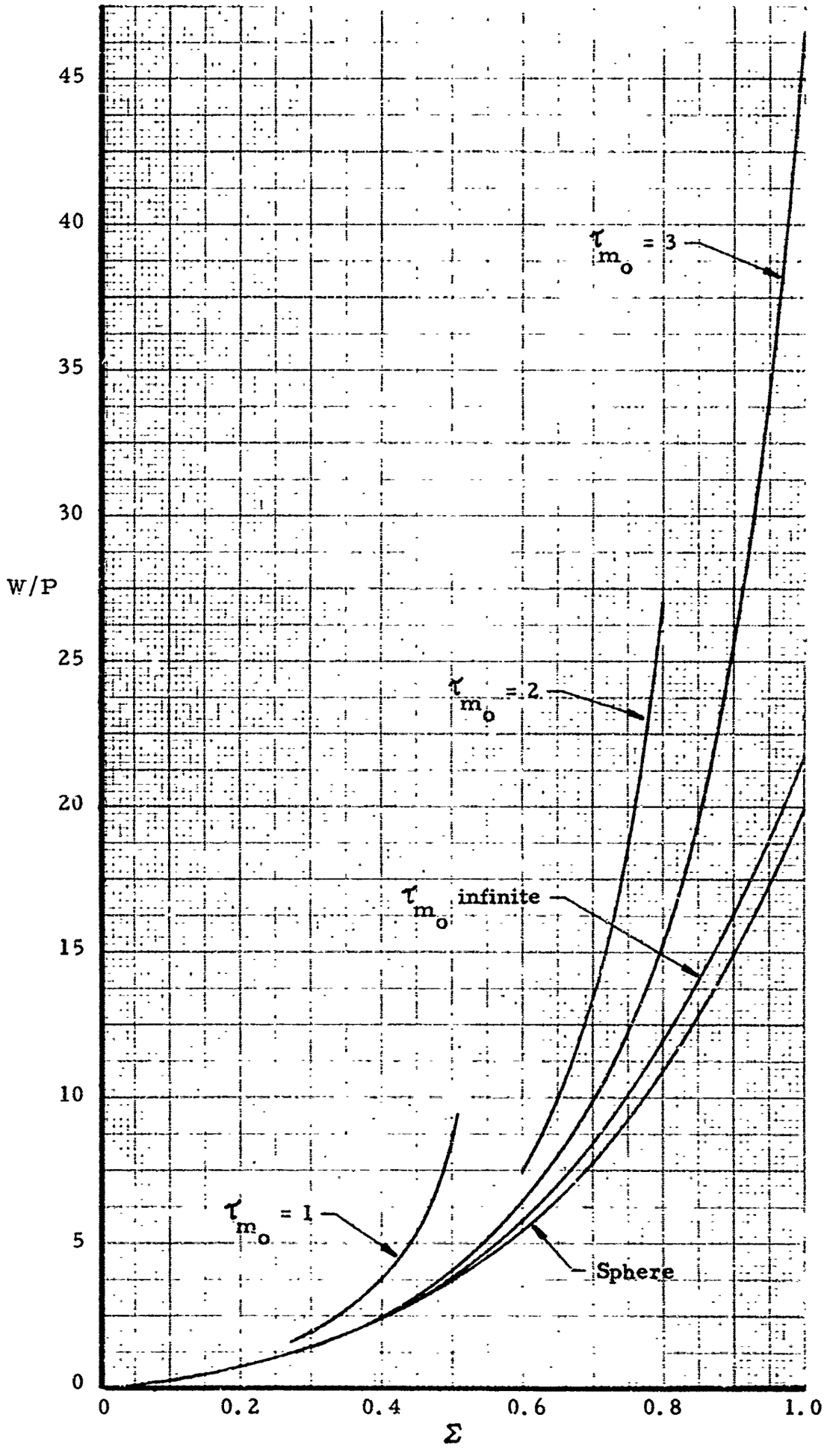

Figure 8. Weight of spherical balloons and of cylinder-end balloons with various values of initial meridional stress
(Zero superpressure, zero circumferential stress)

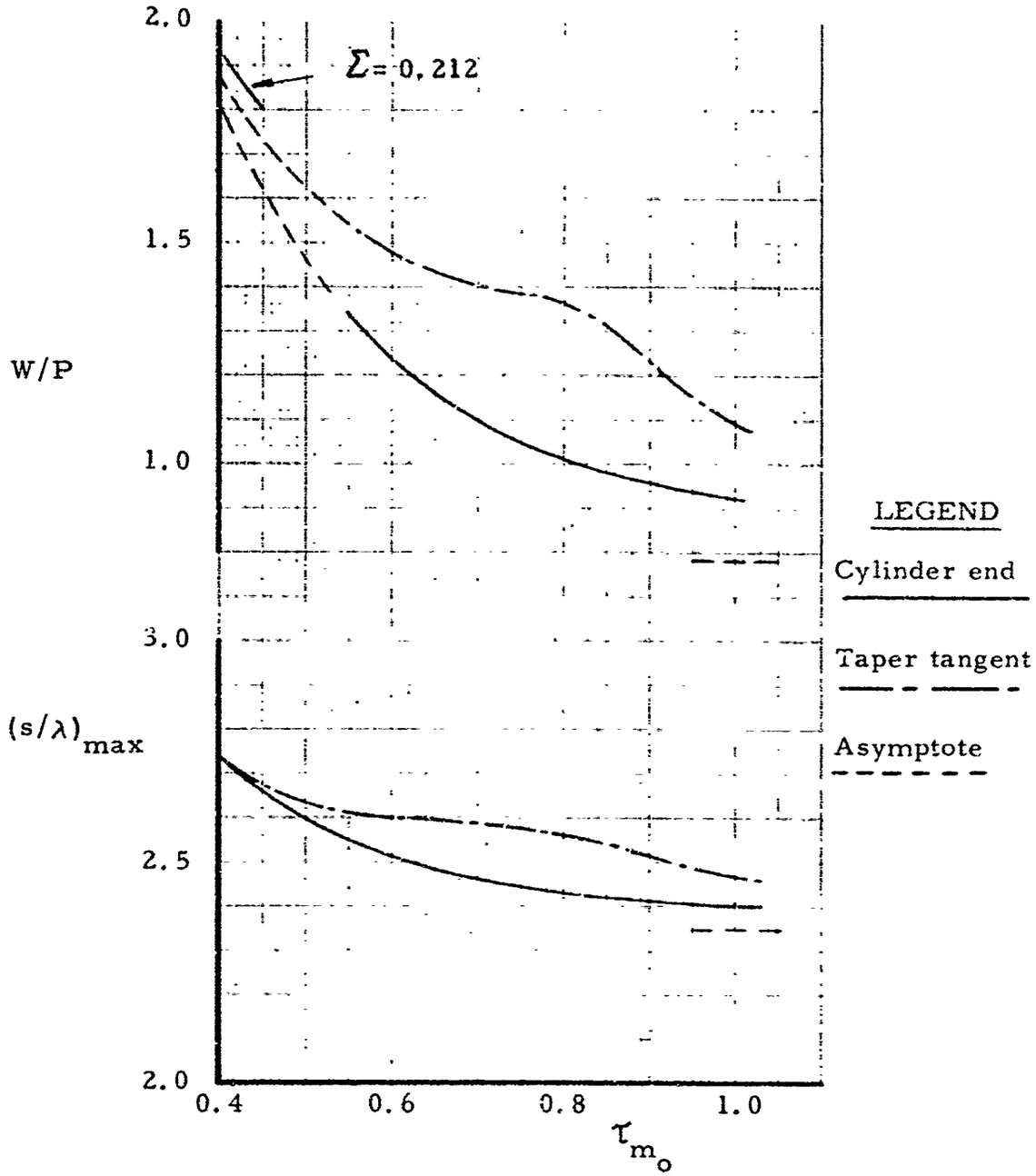

Figure 9. Weight and gore length of balloons with cylinder-end and taper-tangent end sections and varying initial stress (Zero superpressure, zero circumferential stress, $\Sigma = 0.2$)

2. Circumferential Stress Equal to Meridional Stress

Note that it is not possible to have circumferential stress equal to meridional stress at the bottom of the balloon when the payload is applied at a point. Fullness of some kind is required and therefore circumferential stress must be zero. The circumferential stress remains zero until the radius of the balloon exceeds the radius of the end section. At that point in this design, circumferential stress is set equal to meridional stress.

The conditions studied were for zero or low superpressure and for low material stresses. Specifically, in the superpressure range of $0 \leq \alpha \leq 3$ and in the typical polyethylene meridional stress range of $\tau_{m_o} = 1$ or 2, no solutions were found for balloons with a flat top. The sudden change in circumferential stress was the complicating factor. All solutions were either too small--resulting in a peaked top, or too large--resulting in a re-entrant top. There were no intermediate solutions for the conditions studied.

An example of the shape and stress for a balloon with some top loading is shown in Figures 10 and 11. The characteristic inflection in the profile is apparent. The discontinuity in meridional stress is due to the introduction of circumferential stress. Because the meridional stress continues to increase, as opposed to the designs in Figures 4 and 6, the upper cylinder-end section starts immediately above the maximum radius. The weight of this design is $W/P = 0.979$; the load at the bottom is $L/P = 0.685$; the load at the top is $F/P = 0.315$; and the volume is $V/\lambda^3 = 1.979$.

From a practical standpoint it would be better to increase circumferential stress smoothly from its initial zero value. This would permit flat-top solutions at zero superpressure and would probably make it possible to carry the stresses equal to the very top of the balloon.

This design could be an alternate solution to the problem for which the taper-tangent design was evolved.

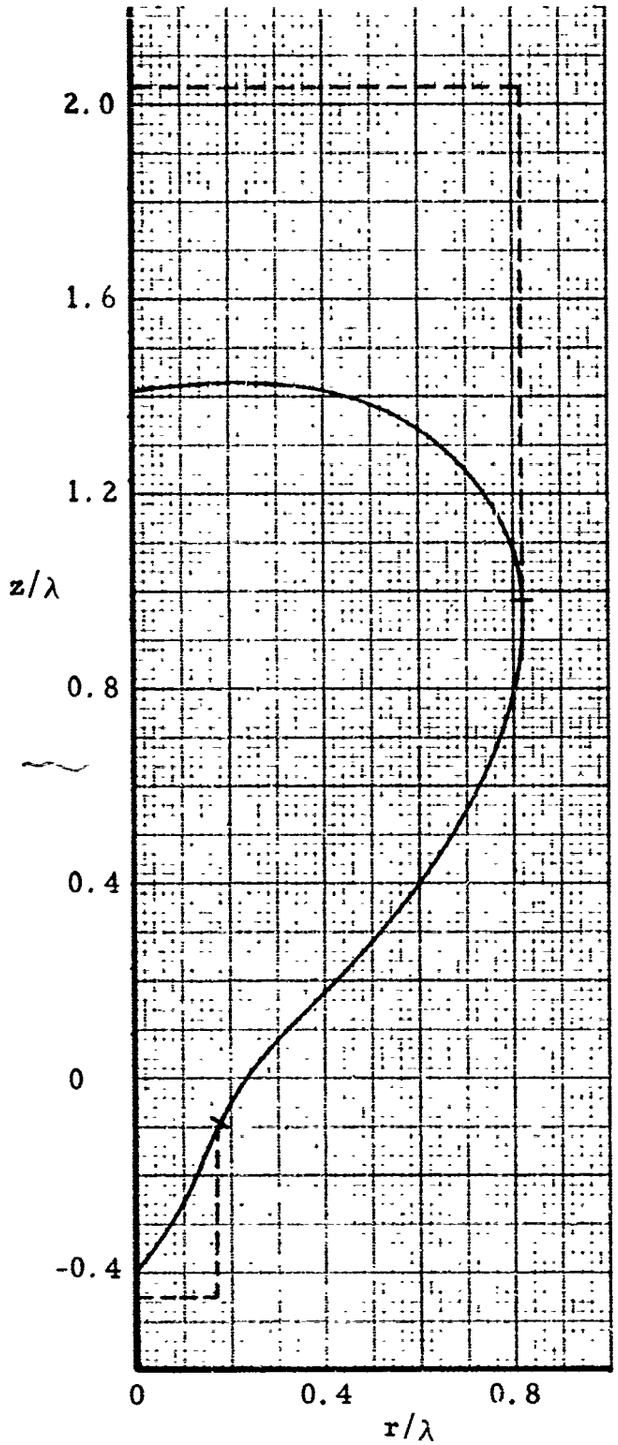

Figure 10. Shape of a cylinder-end balloon with circumferential stress equal to meridional stress in its fully tailored section and equal to zero in its end sections
($\Sigma = 0.176$, $\alpha = 0.882$)
(L/P = 0.685, F/P = 0.315)

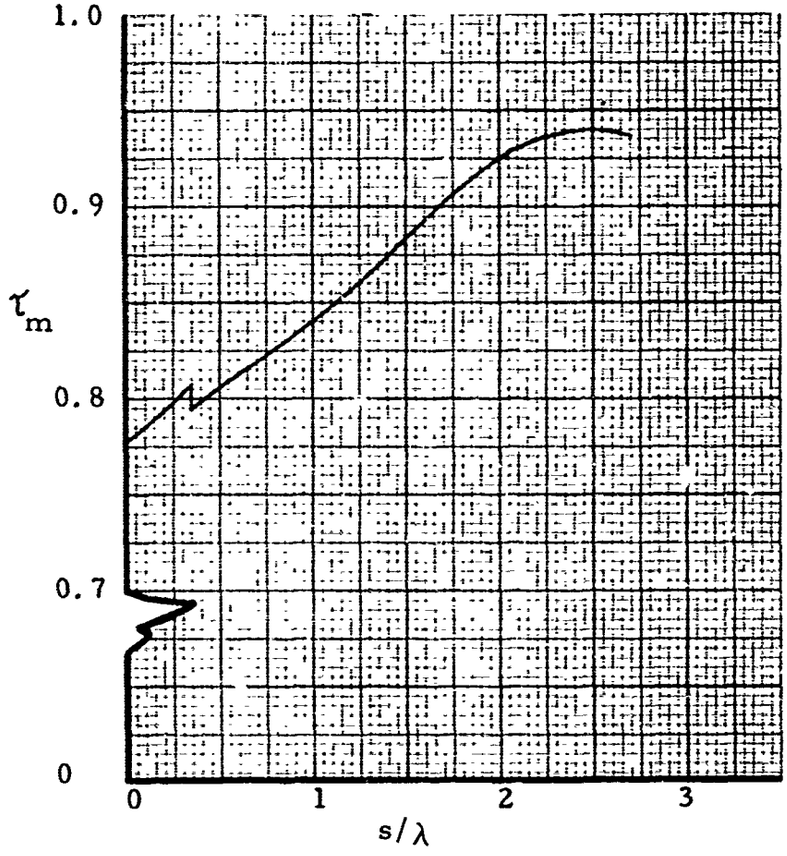

Figure 11. Meridional stress in a cylinder-end balloon with circumferential stress equal to meridional stress in its fully tailored section and equal to zero in its end sections
($\Sigma = 0.176$, $\alpha = 0.882$)
(L/P = 0.685, F/P = 0.315)

B. Taper-Tangent Balloons

Taper-tangent balloons are much like cylinder-end balloons. Thus, examples with only zero circumferential stress are presented here. Figures 12 and 13 show the effect of varying the initial meridional stress for a constant sigma = 0.2. Important differences between these results and the results in Figures 5 and 6 can be noted. In the top of a taper-tangent design, the changeover from the fully tailored section to the end section must occur at a meridional stress value lower than the initial value; otherwise, the final radius will tend to be small and will result in excessive meridional stress. In Figures 12 and 13 the changeover was made arbitrarily when the meridional stress exceeded one-half the initial value. However, when τ_{m_o} equaled 0.8 or less, the meridional stress always exceeded one-half the initial value and the changeover occurred at the first point above the maximum radius.

In general, taper-tangent balloons are heavier than cylinder-end balloons. The gore lengths and weights are shown in Figure 9. Note that when τ_{m_o} is reduced to about 0.4, the taper-tangent and cylinder-end designs merge into the full-cylinder design.

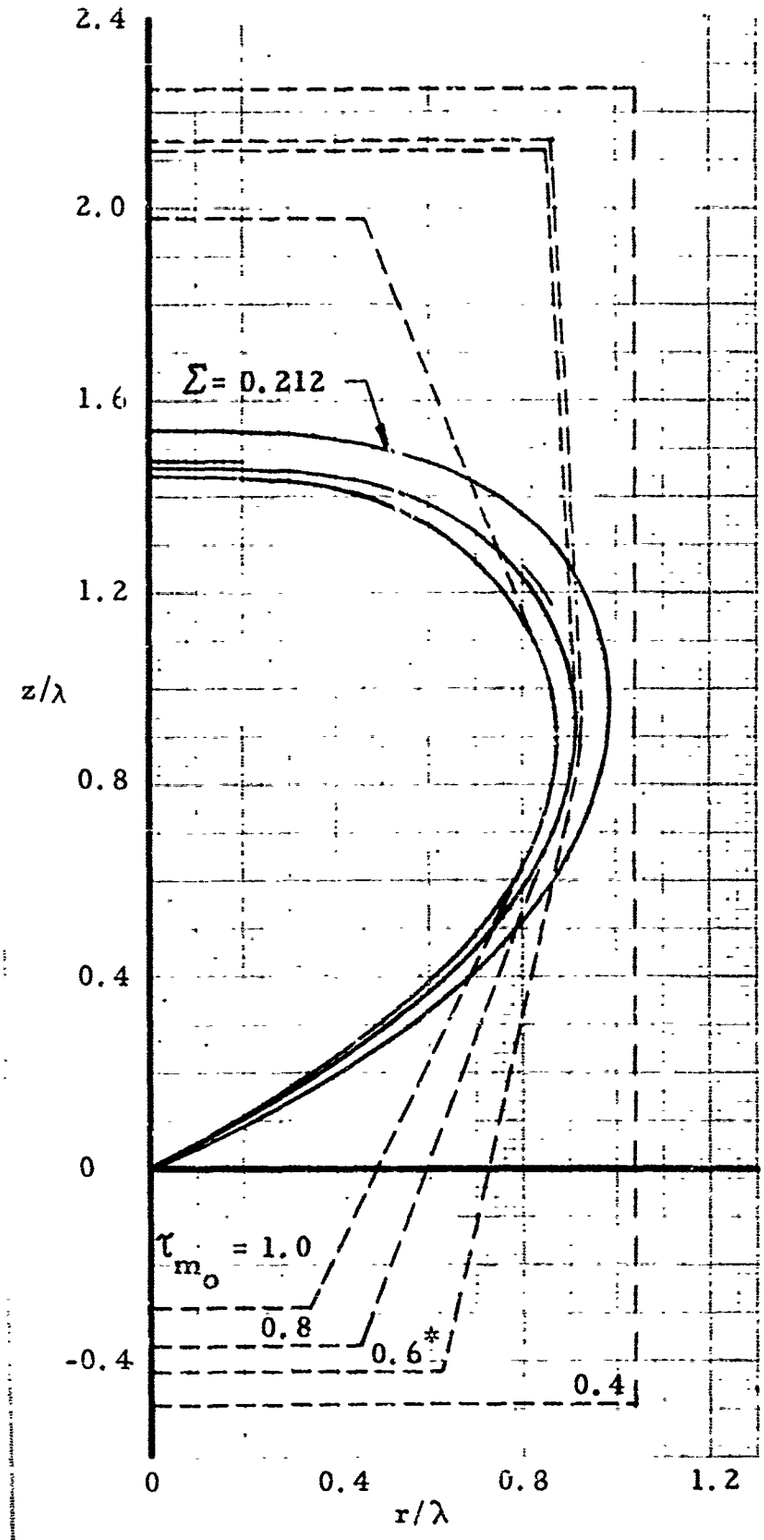

LEGEND

Shape of balloon

Shape of taper-tangent

Figure 12. Shapes of balloons with taper-tangent end sections and varying initial stress (Zero superpressure, zero circumferential stress, $\Sigma = 0.2$)

*(Note: For clarity, the shape for $\tau_{m_o} = 0.6$ is only partially shown.)

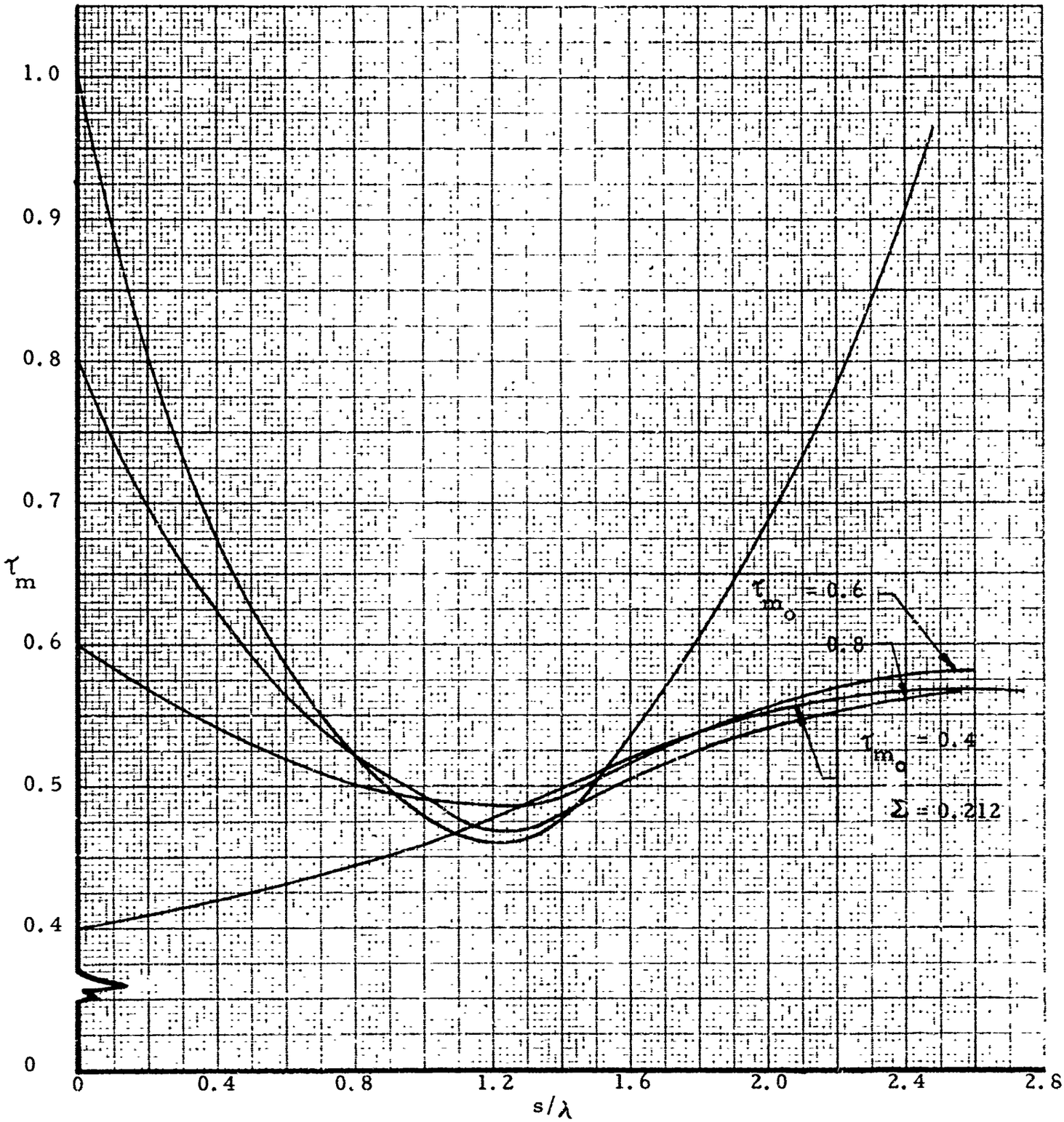

Figure 13. Meridional stress in taper-tangent balloons with varying initial stress (Zero superpressure, zero circumferential stress, $\Sigma = 0.2$)

C. Tangent-Harness Balloons with Meridional and Circumferential Stress Equal

1. Method of Calculation

Considerable difficulty was experienced in determining the shape of these balloons. Rather than closing smoothly at the top, the balloons had re-entrant or peaked tops. Examination of the first of Equations (1c) shows the reason. By re-writing this equation.

$$\frac{d\theta}{ds} = \frac{\cos\theta}{r} - \frac{b(z + a) + w \sin\theta}{t_m}.$$

Usually, z and w are negligible by comparison and t_m is approximately constant. So

$$\frac{d\theta}{ds} \approx \frac{\cos\theta}{r} - \text{a constant.}$$

Cos θ and r are small at the top. So as r decreases, $(\cos\theta)/r$ will tend to become large--the direction depending on the sign of cos θ. Only if all the balloon parameters are chosen correctly will $(\cos\theta)/r$ behave ($\approx$a constant). Divergence at the top is the rule rather than the exception. Trial and error is used to find the proper combinations of parameters. For a particular application, one would usually choose a material weight and desired working stress. By combining these factors with knowledge of the payload, inflation gas, and operating altitude, Σ and initial τ_m become fixed. By varying harness radius and α, a solution can be found wherein the balloon will close at the top with the correct curvature and will have the weight and volume in proper proportion. The top curvature should be

$$-\frac{b(z + a) - w}{2 t_m},$$

where z and t_m are the values at the top. As usual, the weight and volume relationship should be

$$\frac{V}{\lambda^3} = 1 + \frac{W}{P}.$$

2. Numerical Example

The example chosen is for a balloon at 100,000 ft carrying 300 lb. The material weighs 0.0115 lb/ft^2 and the working stress is 174 lb/ft. The lifting gas is helium and the superpressure is 6.34 lb/ft^2. The fixed parameters are:

$\lambda = 68.80$ $\qquad$ $\alpha = 100.0$

$\Sigma = 0.3358$ $\qquad$ $\tau_{m_o} = 40.0$

The shape is very nearly spherical. The ratio of minor and major axes is 0.994. Stresses vary as shown in the following table:

Location	Stress
At Bottom	40.000
At Harness:	
Below	40.004
Above	43.260
At Equator	43.414
At Top	43.570

The weight and volume results are:

$$W/P = 1.69 \text{ and } W = 507 \text{ lb}$$

$$V/\lambda^3 = 2.69 \text{ and } V = 876,000 \text{ ft}^3$$

For the above conditions, it is interesting to see that the harness radius must be about 0.19 (13.1 ft).

VI. REFERENCES

1) General Mills, Inc., Electronics Division.* Report no. 2421. Determination of the shape of a free balloon: Theoretical development, by J. H. Smalley. Contract AF 19(628)-2783. Scientific Report No. 1 (Aug. 2, 1963).

2) ----.* Report no. 2500. Determination of the shape of a free balloon: Balloons with zero superpressure and zero circumferential stress, by J. H. Smalley. Contract AF 19(628)-2783. Scientific Report No. 2 (Dec. 31, 1963).

3) Litton Systems, Inc., Applied Science Division. Report no. 2560. Determination of the shape of a free balloon: Balloons with superpressure, subpressure and circumferential stress; and capped balloons, by J. H. Smalley. Contract AF 19(628)-2783. Scientific Report No. 3 (Apr. 22, 1964).

---

*Information regarding this report may be obtained by contacting the Applied Science Division, Litton Systems, Inc., 2295 Walnut Street, St. Paul, Minnesota 55113.

APPENDIX I

DEFINITION OF SYMBOLS

APPENDIX I

DEFINITION OF SYMBOLS

The symbols used in this series of reports are defined below and illustrated in Figure I-1.

Symbol	Definition	Dimension
a	pressure head at bottom of balloon	length
b	difference in weight densities of air and inflation gas	force per unit volume
k	constant = $(2\pi)^{-1/3}$	
p	gas pressure across the balloon material	force per unit area
r	radial coordinate of a point on balloon, measured normal to the axis of symmetry	length
t_c	circumferential stress in balloon material	force per unit length
t_m	meridional stress in balloon material	force per unit length
t_o, t_l	constants	
s	gore coordinate of a point on the balloon, measured in the meridional direction from the bottom apex	length
w	unit weight of balloon material	force per unit area
z	height coordinate of a point on balloon, measured parallel to the axis of symmetry from the bottom apex	length
A	area of balloon surface	length squared
B	buoyant force on balloon	force
F	vertical load at top apex of balloon	force

G	gross lift of balloon = $b V$	force
L	payload suspended at bottom apex of balloon	force
P	balloon total payload	force
R_c	radius of curvature in the circumferential direction = $r/\cos\theta$	length
R_m	radius of curvature in the meridional plane	length
T	total film load = $2\pi r t_m$	force
V	balloon volume	length cubed
W	balloon weight	force
$\overline{rt}$	$= r t_m/P = \zeta \tau_m$	
α	$= a/\lambda$	
ξ	$= z/\lambda$	
λ	$= (P/b)^{1/3}$	
ρ	$= r/\lambda$	
σ	$= s/\lambda$	
τ	$= t_c/b\lambda^2$	
τ_m	$= t_m/b\lambda^2$	
Σ	$= (2\pi)^{1/3} (w/b\lambda)$	
β	= angle between the balloon material in the end sections and the axis of symmetry--if the end fittings were released and the material fully deployed--measured in a plane containing the axis of symmetry	
Θ	= angle between tangent to the balloon surface and axis of symmetry, measured in a plane containing the axis of symmetry	

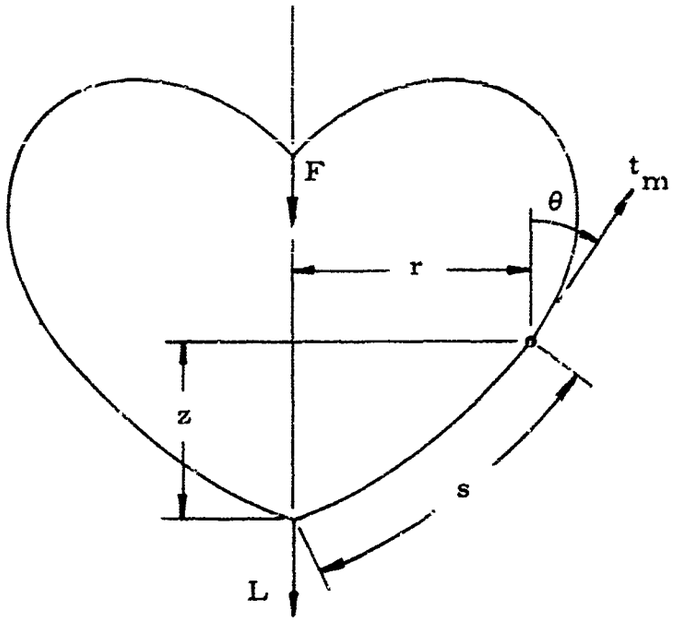

Balloon cross section

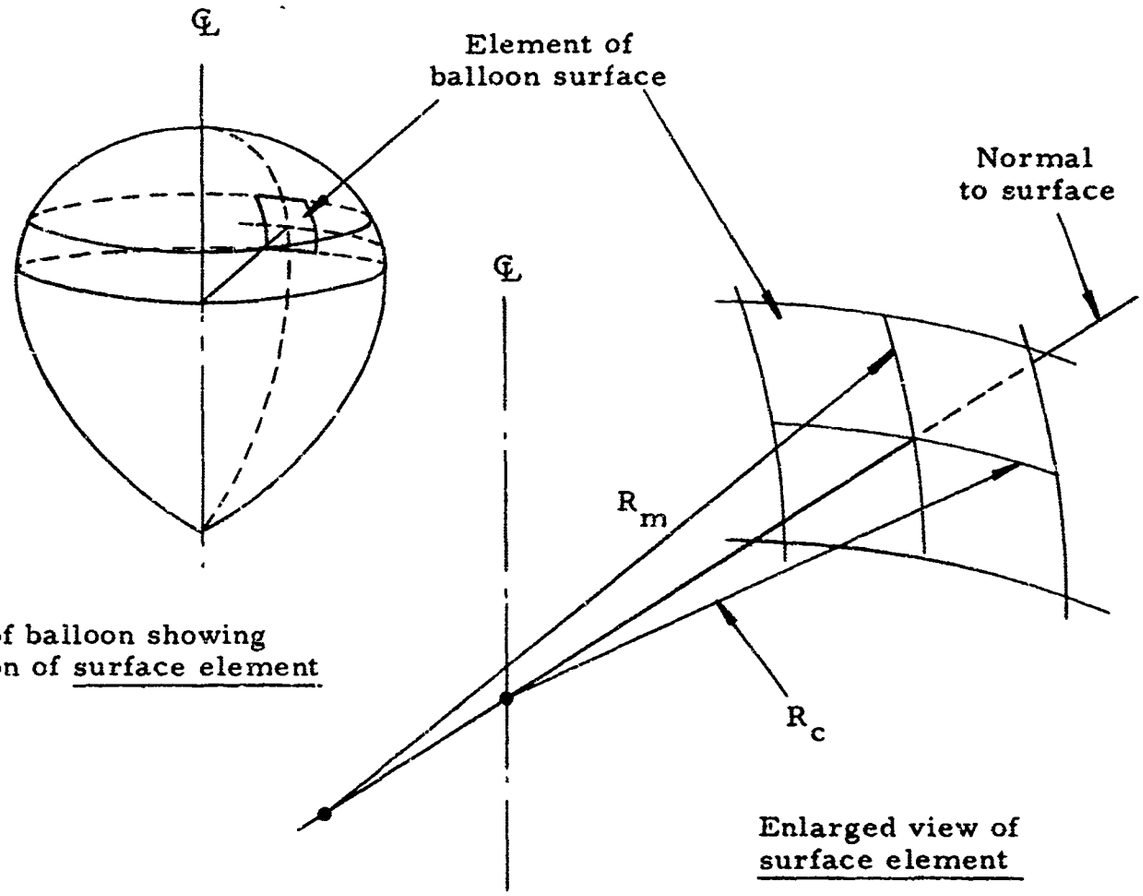

View of balloon showing location of surface element

Enlarged view of surface element

Figure I-1. Pictorial presentation of principal symbols

APPENDIX II

SPHERICAL BALLOONS

APPENDIX II

SPHERICAL BALLOONS

A balloon with minimum possible weight would be perfectly spherical. The volume and gore length of a sphere are derived below in terms of the design parameter (Σ). Symbols are defined in Appendix I.

The gross lift of a balloon is

$$b\,V = W + P.$$

The weight and volume of a sphere are

$$W = 4\pi r^2 w$$

$$V = (4/3)\,\pi r^3;$$

so

$$W = 4\pi w\,(3V/4\pi)^{2/3}.$$

Thus,

$$b\,V = (36\pi)^{1/3}\,(V)^{2/3}\,w + P.$$

By non-dimensionalizing and noting that

$$P = b\,\lambda^3$$

$$k\Sigma = w/b\,\lambda,$$

we have

$$\frac{V}{\lambda^3} = 1 + (18)^{1/3} \sum \left(\frac{V}{\lambda^3}\right)^{2/3} . \qquad \text{(II-1)}$$

The weight, as usual, is

$$\frac{W}{P} = \frac{V}{\lambda^3} - 1 .$$

The volume is conveniently solved for by iteration. Let

$$y^3 = \frac{V}{\lambda^3};$$

then Equation (II-1) becomes

$$y^3 = 1 + (18)^{1/3} \sum y^2 . \qquad \text{(II-2)}$$

Also let

y_1 = an approximate solution to (II-2)

y_2 = a better approximate solution to (II-2)

x_1 = the value of $\sum$ for which y_1 would be a solution

$$(18)^{-1/3} \left(y_1 - \frac{1}{y_1^2}\right) .$$

Then by Newton's method,*

$$y_2 = y_1 + \frac{\sum - x_1}{\frac{3}{(18)^{1/3}} - \frac{2 x_1}{y_1}} .$$

---

*Scarborough, J. B. Numerical mathematical analysis, third ed Baltimore Johns Hopkins Press, 1955.

The gore length of a sphere

$$s = \pi r.$$

By introducing the sphere weight,

$$s^2 = \frac{\pi}{4} \frac{W}{w} .$$

Then by non-dimensionalizing,

$$\left(\frac{s}{\lambda}\right)^2 = \frac{1}{2}\left(\frac{\pi^4}{4}\right)^{1/3} \left(\frac{W}{P}\right)\left(\frac{1}{\Sigma}\right).$$

Results for volume, gore length and other physical characteristics are shown in Table II-1.* When $\Sigma = 0$, the gore length is determined by our knowledge of V/λ^3. By combining volume and gore length,

$$V = \frac{4}{3}\frac{s^3}{\pi^2};$$

or

$$\frac{V}{\lambda^3} = \frac{4}{3\pi^2}\left(\frac{s}{\lambda}\right)^3.$$

But when $\Sigma = 0$,

$$\frac{V}{\lambda^3} = 1;$$

---

*A simple check of Table II-1 will show that the various powers of gore length and volume are not mutually compatible (e.g., for $\Sigma = 1.0$, $(2.75271)^3 \neq 20.85847$). However, the data in the table are correct; each number was computed to a accuracy greater than is shown and rounded off to five decimal places.

TABLE II-1

NON-DIMENSIONAL PHYSICAL PARAMETERS OF SPHERICAL BALLOONS

SIGMA	RADIUS	AREA	GORE LENGTH	$\left(\text{GORE LENGTH}\right)^2$	$\left(\text{GORE LENGTH}\right)^3$	$(\text{VOLUME})^{1/3}$	$(\text{VOLUME})^{2/3}$	VOLUME
0.00	0.62035	4.83598	1.94889	3.79817	7.40220	1.00000	1.00000	1.00000
0.05	0.64866	5.28750	2.03784	4.15279	8.46273	1.04564	1.09337	1.14327
0.10	0.67955	5.80301	2.13487	4.55768	9.73005	1.09543	1.19997	1.31448
0.15	0.71320	6.39200	2.24059	5.02026	11.24838	1.14968	1.32176	1.51960
0.20	0.74980	7.06477	2.35556	5.54866	13.07020	1.20867	1.46088	1.76572
0.25	0.78948	7.83226	2.48021	6.15145	15.25688	1.27263	1.61958	2.06113
0.30	0.83233	8.70573	2.61485	6.83746	17.87898	1.34172	1.80020	2.41536
0.35	0.87842	9.69639	2.75962	7.61553	21.01600	1.41600	2.00505	2.83915
0.40	0.92770	10.81503	2.91446	8.49411	24.75577	1.49545	2.23637	3.34438
0.45	0.98012	12.07162	3.07913	9.48103	29.19331	1.57994	2.49621	3.94387
0.50	1.03552	13.47502	3.25319	10.58326	34.42938	1.66926	2.78641	4.65123
0.55	1.09374	15.03279	3.43609	11.80672	40.56898	1.76310	3.10853	5.48066
0.60	1.15456	16.75108	3.62716	13.15627	47.71984	1.86114	3.46385	6.44671
0.65	1.21775	18.63473	3.82566	14.63568	55.99114	1.96300	3.85335	7.56412
0.70	1.28306	20.68733	4.03086	16.24779	65.49250	2.06828	4.27780	8.84770
0.75	1.35027	22.91146	4.24201	17.99462	76.33328	2.17663	4.73771	10.31224
0.80	1.41916	25.30880	4.45842	19.87749	88.62214	2.28767	5.23344	11.97240
0.85	1.48951	27.88040	4.67945	21.89722	102.46684	2.40108	5.76521	13.84275
0.90	1.56115	30.62678	4.90451	24.05421	117.97413	2.51657	6.33311	15.93770
0.95	1.63391	33.54809	5.13309	26.34861	135.24977	2.63385	6.93719	18.27156
1.00	1.70765	36.64425	5.36473	28.78032	154.39865	2.75271	7.57743	20.85847

so

$$\left(\frac{s}{\lambda}\right)^3_{\Sigma=0} = \frac{3\pi^2}{4} = 7.402203301,$$

and

$$\left(\frac{s}{\lambda}\right)_{\Sigma=0} = 1.94889$$

$$\left(\frac{s}{\lambda}\right)^2_{\Sigma=0} = 3.79817.$$

For comparison, the weight of spherical balloons is plotted in Figure 8.